A Novel Active Damping Mechanism for Multi-Chambered Parallel Soft Robots

Ameer Hamza Khan, Zili Shao, Shuai Li

***Abstract*—Fabricated using silicones, soft robots, are highly elastic systems with the advantage of inherent flexibility, compliance, and safety in human interaction. However, because of their flexible bodies, they oscillate vigorously, when deactuated, before settling down. These oscillations might compromise the structural integrity of soft robot with time. So far, there is a very little investigation on the passive and active oscillation damping methods for the soft robots. In this work, we present the design of a 6-chambered parallel soft robot and propose an effective active damping method by a smart distribution of the 6 actuation chambers. Experimental verification of the effectiveness of the proposed damping method is conducted on the proposed parallel soft robot. It is shown that the proposed method provides a high degree of oscillation damping thus prolonging the actuator life. Since the proposed method uses the components of the soft robot itself to actively create oscillation damping, there is no additional mechanical overhead.**

I. Introduction

Soft robots have attracted a great research attention in recent years and have demonstrated their potential application in practical systems [1], [2]. Most of the practical applications require the robots to be fast and steady [3]. High speed increases productivity while steadiness reduces undesirable effects e.g. overshooting, vibrations. For traditional rigid robots, such undesirable effects are naturally reduced due to use of stiff materials and rigorously studied control methods to provide active damping [4]. On the other hand, owing to their flexible bodies, soft robot usually exhibit large oscillations on deactuation or a sudden change in the control signal. Soft robots are inspired by soft-bodied animals existing in nature e.g. worms, octopus etc [5]. They can easily locomote and interact with the irregular environment due to their flexible and compliant structure, without causing any damage to the environment [6]. Whereas, traditional rigid robots require complex sensing mechanisms and advanced control theory to safely interact with delicate objects. Soft robots offer great promises in simplifying the problem of safe human-robot interaction. But the problem posed by the oscillations need to be addressed.

Soft Pneumatic Actuators (SPAs) [7], [8] are the most common type of soft actuator which have been widely studied and applied in industrial and rehabilitation applications [1], [2]. These actuators use pneumatics for actuation and gained popularity because of their fast response rate, simple design, ease of fabrication, and low cost. SPAs consist of several inflatable chambers and actuation is produced by inserting high-pressure air into these chambers. High-pressure increase chamber volume producing motion in the SPA. Several different designs of SPAs are proposed in literature i.e. linear actuators [9], bending actuators [8], [10]. In this paper, we consider a 6-chambered parallel soft robot as shown in Fig. 1.

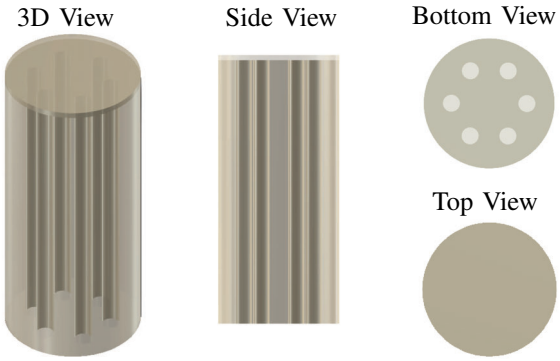

Fig. 1: 3D model of the 6-chambered parallel soft robot. Left: 3D view of the model, top right: side view, and bottom right: bottom view of the soft robot model.

Despite the advantages offered by soft robots as compared to the traditional rigid robots, they also pose several challenges. Most important among those challenges is accurate and robust control of the motion of soft robots. Since soft robots are made entirely of soft materials, their flexible structure undergo large overshoot and oscillations when suddenly deactuated at high-pressure air. These oscillations happen because, in the absence of any external damping, the natural stiffness of the flexible material is very small. Fig. 2 shows the oscillations amplitude caused deactuation. The oscillations have an amplitude of about 20 degrees and settling time of about 0.9 seconds. Such large oscillations in the soft robot will not only reduce their viability and efficiency in industrial applications but can also cause undesirable effects such as an increase in operating time, damage to the delicate objects present in surrounding of the soft robot, and cause wear and tear of soft robot reducing the lifetime. These characteristics will greatly impact their usefulness in time-critical industrial applications, where accuracy and robustness are of utmost importance.

Mechanical system dissipates their kinetic and potential energy, because of damping, in the form of heat when deactuated. Every material has internal damping depending on its stiffness e.g. rigid materials have high damping as compared to soft material [11]. For soft materials, the internal damping is not enough to suppress oscillations. An external damping method needs to be used to achieve the desired level of oscillation damping and quick steady-state stabilization. External damping is further classified into passive and active

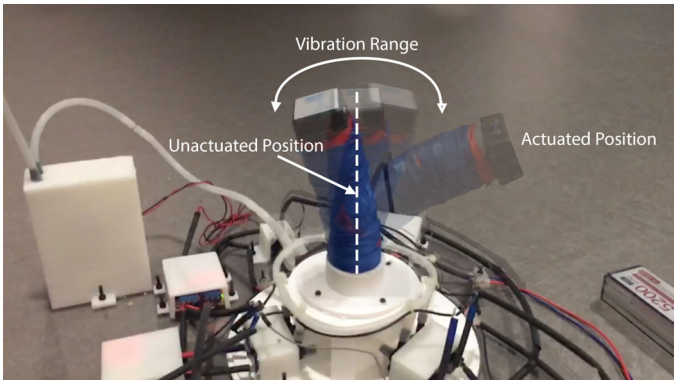

Fig. 2: The oscillations produced in soft robot on deactuation.

damping [11]. Ni et al. [12], [13] propose a passive damping technique by attaching an additional mechanical damper along with the soft robot. The proposed method is able to provide the desired level of damping but the use of additional components make the system bulky. Active damping method includes the active use of actuation signal to create damping effect. Li et al. [14] proposes the use of a seperate partical chamber attached to the soft robot. The damping is created by applying a negative vaccum suction pressure to the particle chamber. The particle chamber augment the energy discsipation by creating frictional and collision forces.

In this work, we propose an active damping approach by smartly distributing the inflatable chambers in the body of the soft robot. The design of the proposed 6-chambered parallel soft robot shown in Fig. 1. The soft robot consists of 6 linear empty chambers symmetrically distributed in the circular pattern inside the soft robots body. When a chamber is inflated, the volume of that chamber increases, forcing the soft robot to bend in the opposite direction. Note that, in absence of any active damping, the chamber radially opposite to the actuated chamber will always be deactuated. If both radially opposite chambers are actuated together, they will cancel each others bending effect. We leverage this cancellation property of radially opposite chambers to create active oscillation damping during actuation and deactuation.

The rest of the paper is distributed as follow: Section II describes the design, fabrication, actuation and sensing mechanism of the 6-chambered parallel soft robot, section III describes the experimental platform and evaluation methodology, section IV presents the experimental results with V concluding the paper.

II. Soft Robot Design and Damping Mechanism

In this section, the design, fabrication, sensing and actuation mechanism of the 6-chambered parallel soft robot.

A. Actuator Design

The previous works [12]–[14] on soft robot oscillation damping add additional mechanical components, to create active or passive damping. In this work, we propose a novel design of the soft actuator such that the different components of the soft robots are capable of generating damping for each other, without any additional mechanical overhead. The 3D design of the proposed 6-chambered parallel soft robot as shown in Fig 1. The parallel soft robot has a cylindrical soft body, embedding six parallel linear chambers. The linear chambers are distributed evenly in a circular pattern inside the body of the soft robot. The key to the active damping lies in distributing the chambers in a circular pattern so that radially opposite chambers will provide oscillation damping by motion cancellation effect as explained later in this section. One end of the cylindrical soft robot is fixed to a solid base. In deactuated state, the soft robot remains vertical. When one of the chambers is actuated, the volume of that chamber increases and the soft robot bend in the opposite direction.

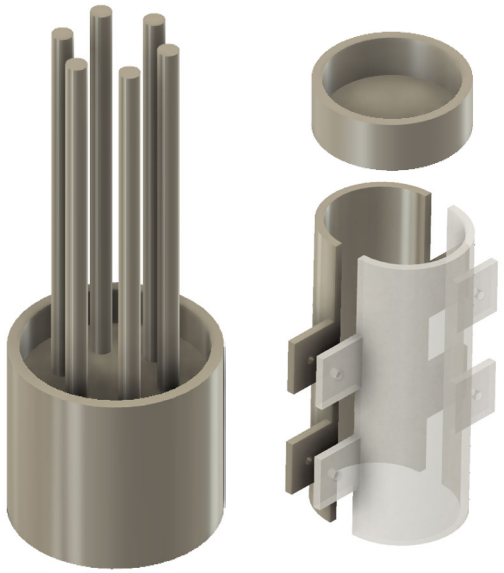

Fig. 3: 3D drawing of the molds used to cast the 6-chambered parallel soft robot. Left: base of the mold, top right: cap of the mold, and bottom right: the wall to be inserted in mold base.

The soft robot was fabricated using Dragon Skin 30 [15] silicone. The length and outer radius of the soft robot are 10cm and 4cm respectively, whereas the radius of each inner chamber is 5mm. We designed the molds as shown in Fig. 3. The liquid silicone was poured in 3D printed molds and allowed to be cured in the open air for about 8 hours. After curing of silicone was complete, the solidified soft robot was removed from the molds. The robot is wrapped in fabric to prevent the damage to the soft robot on a sudden application of high air pressure.

B. Soft Robot Model

The soft actuator design presented in the last section consists of 6 chambers. The chambers are evenly distirbuted along the circumference of the soft robot in a circular pattern. When a single channel is actuated, the soft robot produce a simple bending motion. This bending motion of the soft robot can be expressed in term of the bending angle θ of its top surface relative to its initial horizontal position. The bending angle θ is related to the air pressure P inside the air chamber. The

relation between P and θ can be drived using the Lagrangian $\mathbb{L}$ of the soft robot. The Lagrangian of a system is defined as

$$\mathbb{L} = \mathbb{T} - \mathbb{V}, \tag{1}$$

where $\mathbb{T}$ is the total kinetic energy and $\mathbb{V}$ is the potential energy present in the system. Using the Lagrangian $\mathbb{L}$ the dynamic equation of the system can be defined as

$$\frac{d}{dt}\frac{\partial \mathbb{L}}{\partial \dot{\theta}} - \frac{\partial \mathbb{L}}{\partial \theta} = \tau - b\dot{\theta}, \tag{2}$$

where τ is the generalized input force and b models the frictional forces preent in the system.

The total potential energy $\mathbb{V}$ of the system is mainly contributed by the elastic potential energy. The elastic potential energy of a deformable system is given by the following relation

$$\mathbb{V} = \frac{1}{2}VE\epsilon^2, \tag{3}$$

where E is the Young's modulus, V is the volume of the material undergoing deformation and ϵ is the strain present in the soft robot as the result of bending motion. As shown in [16], the relation between strain ϵ and bending angle θ can be approximated to be linear for soft bending robots i.e. $\epsilon = k\theta$, where k is a constant of proportionality. Therefore the total potential energy of the system can be expressed as

$$\mathbb{V} = \frac{1}{2}VEk^2\theta^2.$$

The generalized input force τ is given by $\partial\mathbb{V}/\partial\theta$, using relation (3)

$$\tau = VEk^2\epsilon.$$

Since the actual physical input to the system is air pressure P, we are interested in the relation of generalized force τ in term of P. As shown by [17] the strain produced in a bending soft robot is directly proportional to its internal air pressure P i.e. $\epsilon = cP$. Here c is a constant of proportionality between strain ϵ and air pressure P. Therefore

$$\tau = VEcP.$$

Now we will calculate the total kinetic energy $\mathbb{T}$ present in the system. The total kinetic energy is mainly contributed by the rotational kinetic energy of the soft robot

$$T = \frac{1}{2}I\dot{\theta}^2,$$

where I is the rotational inertia of the soft robot. Replacing the derived values of $\mathbb{T}$ and $\mathbb{V}$ in (1), the lagrangian becomes

$$L = \frac{1}{2}I\dot{\theta}^2 - \frac{1}{2}VEk^2\theta^2.$$

Putting the values of $\mathbb{L}$ and τ in (2), we get

$$I\ddot{\theta} + VEk^2\theta = VEcP - b\dot{\theta}.$$

Thus the dynamic model of the soft robot is given by

$$VEk^2\theta + b\dot{\theta} + I\ddot{\theta} = VEcP.$$

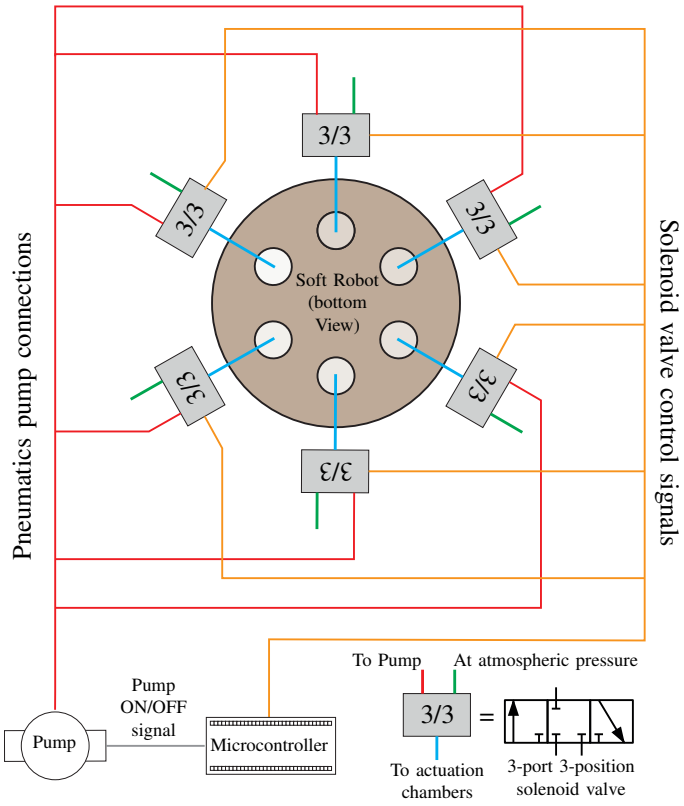

Fig. 4: Schematic diagram of the actuation mechanism developed for the parallel soft robot used in our experiments.

This relation models the motion dynamics of the soft robot when a single chamber is actuated. Our parallel soft robot have a total of six identical chambers, therefore similar motion dynamics can be applied to each chamber, although in a rotated reference frame. The multiple chamber actuation can be calculated by superposition of individual chamber actuation.

C. Actuation And Sensing

The actuation principle of the 6-chambered parallel soft robot is shown in Fig. 4. All six chambers inside the soft robot are connected with the air pump through 3-port 3-position solenoid valves. The 3 ports of each valve are connected as: one output port is connected with one of the chambers of the soft robot and the other two ports are connected with the air pump and atmospheric pressure respectively. The 3 positions of the solenoid valves correspond to inward flow, hold the air inside the chamber and outward flow. The solenoid valves cannot be directly driven through microcontroller pins because of the high current requirement. Therefore, the solenoid valves are driven through MOSFET switches, which in turn are controlled through a microcontroller. The expansion of any chamber in the soft robot is proportional to the inward flow duration of the air i.e. the opening time of the solenoid valve.

We used an orientation sensor for measurement of the bending angle. The sensor was mounted on the top of the soft robot. The orientation sensor is used to estimate the amplitude of the oscillation and settling time of the soft robot. Although in this study we are just concerned about vibration damping of

radially opposite chambers, the orientation sensor is capable of measuring 3D rotations of the top surface of the soft robot.

D. Damping Mechanism

As already explained in section II-A, the previous work in soft robot oscillation damping adds additional mechanical components overhead. In our work, we propose a novel design of the soft actuator, in which the damping effect is achieved by the smart distribution of inflating chambers inside the soft robots. In our 6-chambered parallel soft robot, the number of linear chambers was chosen to be even i.e. six, so that on the circular distribution of chambers, there is always a chamber radially opposite to another chamber i.e. there are always two chambers at 180 degree from each other as shown in Fig. 4. To understand the damping mechanism, refer to Fig. 5. For simplicity and ease of explanation, the image just shows 2D planner motion. Suppose, in the current state, the left chamber of the soft robot is actuated and the current pose of the top surface of the soft robot is rightward at an angle of 45 degrees. On deactuation, it will return to vertical position i.e. top surface angle becomes 0. This will require the deflation of the left chamber creating a leftward bending force. If there is no active damping, this force will bend the actuator to the vertical position but with oscillations. Now consider simultaneous actuation of the right chamber, but for a very small period of time. This actuation of the right chamber will produce a smaller rightward bending force. Since the right chamber is actuated only for a smaller duration, the pressure developed inside it will be smaller as compared to deactuation pressure of the left chamber. The net force is still leftward, but the little rightward force is sufficient enough to create oscillation damping effect. The amount of damping is dependent on the ratio of right chamber deactuation pressure and left chamber actuation pressure and is defined as

$$\delta = \frac{\text{damping Actuation Pressure}}{\text{Deactuation Pressure}} \tag{4}$$

where δ is damping actuation ratio, and its effect on oscillation damping is analyzed in the Results section.

III. Experimental Platform

The experimental platform constructed to perform the experiments is shown in Fig. 6. The experimental platform consists of a strong plastic base, on which the soft robot was mounted vertically. All the pneumatics, electrical and electronics systems are attached to the base of the plastic platform, to make the system portable. We used six 3-port 3-position solenoid valves i.e. one for each chamber inside the soft robot. We used an Arduino Uno as the controller board, for sensor data acquisition and processing. To collect vibration information, we used a 3-axis orientation sensor which gives 3D rotations (i.e. roll, pitch, and yaw) of the top surface. The sensor is glued to the top of the soft robot. The orientation sensor was connected to the Arduino Uno using Bluetooth connection. The 3-port 3-position solenoid needs to be driven by high current, which Arduino Uno pins cannot drive directly. To isolate the microcontroller pins from the solenoid valves,

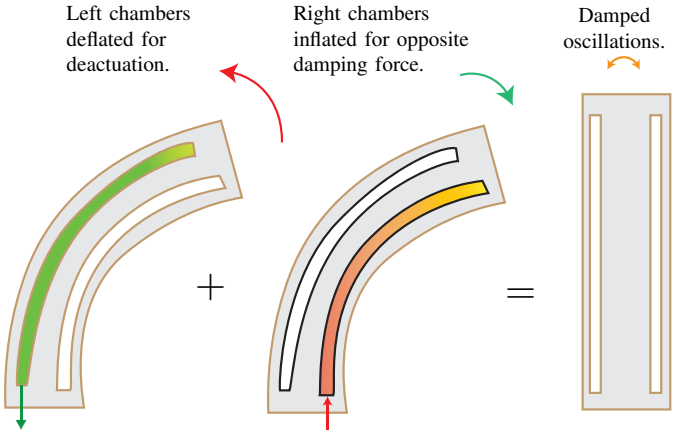

Fig. 5: 2D illustration of the active oscillation damping mechanism during deactuation. The daming force is created by simultaneous deactuation of left chamber and actuation of right chamber.

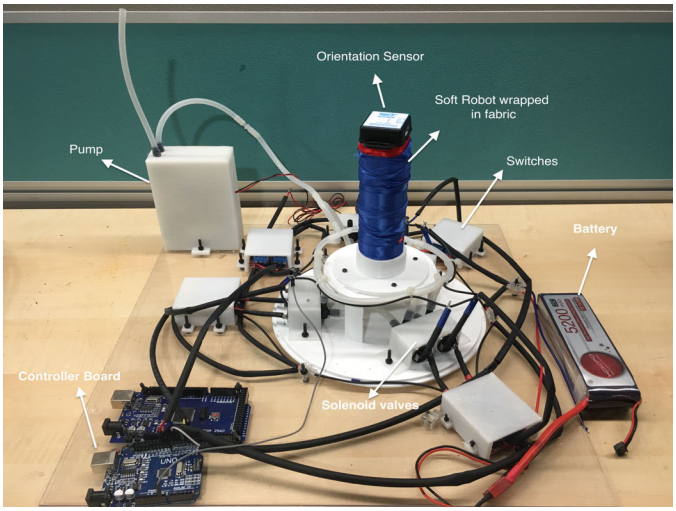

Fig. 6: Experimental Platform developed to demonstrate the effectiveness of the proposed oscillation damping method.

we used MOSFET switches. These switches are capable of providing high current required to drive the solenoid valves.

IV. Experimental Results

In this section, we will report the experimental results to verify the effectiveness of the proposed active oscillation damping method. We will also analyze the effect of damping actuation ratio (δ) defined in (4). Fig. 7 sshows that oscillation profiles under different damping actuation ratio. It can be seen that in the absence of any active damping, the soft robot produce quite large oscillations (about 18 degrees peak value) and settles down to the deactuated position after about 1 second. But when we start to apply the active oscillation damping mechanism as explained in section II-D the oscillation amplitude began to decay and the settling time becomes small. It can be seen that the decrease in the oscillation magnitude and settling time is directly proportional to the damping actuation ratio (δ). It is also worth considering that after damping actuation

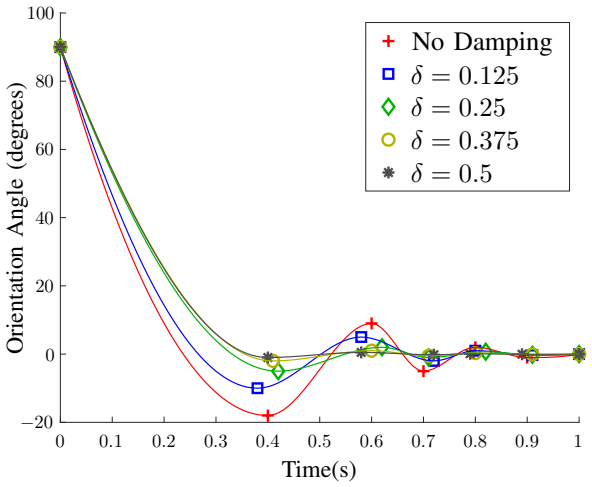

Fig. 7: Oscillation profile of the soft robot with no damping compared with the active oscillation damping.

ratio becomes sufficiently large (about 0.5), the system even starts to behave like a nearly overdamped system. The peak oscillation magnitude reduces to a mere 2 degrees and settling time reduces to 0.5 seconds. The demonstration of active oscillation damping can be seen at video available on this link: https://www4.comp.polyu.edu.hk/~csahkhan/damping.mp4

V. Conclusion

In this paper, we presented a novel active damping approach for soft robots, by a smart distribution of actuation chambers inside the soft robot body. The approach leverage the structure of soft robot itself to actively create damping effect, therefore, requires no additional mechanical and electrical overhead. We proved the efficacy of the proposed method by experimental results.

References

[1] H. Lin, F. Guo, F. Wang, and Y.-B. Jia, "Picking up a soft 3d object by feeling the grip," *The International Journal of Robotics Research*, vol. 34, no. 11, pp. 1361–1384, 2015.

[2] P. Polygerinos, S. Lyne, Z. Wang, L. Nicolini, B. Mosadegh, G. Whitesides, and C. Walsh, "Towards a soft pneumatic glove for hand rehabilitation," in *Intelligent Robots and Systems (IROS), 2013 IEEE/RSJ International Conference on*, pp. 1512–1517, IEEE, 2013.

[3] J. W. Jeon, "An efficient acceleration for fast motion of industrial robots," in *Industrial Electronics, Control, and Instrumentation, 1995., Proceedings of the 1995 IEEE IECON 21st International Conference on*, vol. 2, pp. 1336–1341, IEEE, 1995.

[4] E. Pereira, S. S. Aphale, V. Feliu, and S. R. Moheimani, "Integral resonant control for vibration damping and precise tip-positioning of a single-link flexible manipulator," *IEEE ASME Transactions on Mechatronics*, vol. 16, no. 2, p. 232, 2011.

[5] C. Laschi, M. Cianchetti, B. Mazzolai, L. Margheri, M. Follador, and P. Dario, "Soft robot arm inspired by the octopus," *Advanced Robotics*, vol. 26, no. 7, pp. 709–727, 2012.

[6] A. D. Marchese, R. K. Katzschmann, and D. Rus, "A recipe for soft fluidic elastomer robots," *Soft Robotics*, vol. 2, no. 1, pp. 7–25, 2015.

[7] Y. Yang, Y. Chen, Y. Li, M. Z. Chen, and Y. Wei, "Bioinspired robotic fingers based on pneumatic actuator and 3d printing of smart material," *Soft robotics*, vol. 4, no. 2, pp. 147–162, 2017.

[8] B. Mosadegh, P. Polygerinos, C. Keplinger, S. Wennstedt, R. F. Shepherd, U. Gupta, J. Shim, K. Bertoldi, C. J. Walsh, and G. M. Whitesides, "Pneumatic networks for soft robotics that actuate rapidly," *Advanced functional materials*, vol. 24, no. 15, pp. 2163–2170, 2014.

[9] M. Doumit, A. Fahim, and M. Munro, "Analytical modeling and experimental validation of the braided pneumatic muscle," *IEEE transactions on robotics*, vol. 25, no. 6, pp. 1282–1291, 2009.

[10] P. Polygerinos, Z. Wang, J. T. Overvelde, K. C. Galloway, R. J. Wood, K. Bertoldi, and C. J. Walsh, "Modeling of soft fiber-reinforced bending actuators," *IEEE Transactions on Robotics*, vol. 31, no. 3, pp. 778–789, 2015.

[11] C. W. De Silva, *Vibration damping, control, and design*. CRC Press, 2007.

[12] F. Ni, A. Henning, K. Tang, and L. Cai, "Soft damper for quick stabilization of soft robotic actuator," in *Real-time Computing and Robotics (RCAR), IEEE International Conference on*, pp. 466–471, IEEE, 2016.

[13] Y. Wei, Y. Chen, T. Ren, Q. Chen, C. Yan, Y. Yang, and Y. Li, "A novel, variable stiffness robotic gripper based on integrated soft actuating and particle jamming," *Soft Robotics*, vol. 3, no. 3, pp. 134–143, 2016.

[14] Y. Li, Y. Chen, T. Ren, and Y. Hu, "Passive and active particle damping in soft robotic actuators," in *Robotics and Automation (ICRA), 2018 IEEE International Conference on*, pp. 1547–1552, IEEE, 2018.

[15] "Smooth-on inc." https://www.smooth-on.com/tb/files/DRAGON_SKIN_SERIES_TB.pdf. Accessed: 2018-08-28.

[16] A. Marchese, R. Tedrake, and D. Rus, "Dynamics and trajectory optimization for a soft spatial fluidic elastomer manipulator," *The International Journal of Robotics Research*, vol. 35, no. 8, pp. 1000–1019, 2016.

[17] B. Tondu and P. Lopez, "Modeling and control of mckibben artificial muscle robot actuators," *IEEE control systems*, vol. 20, no. 2, pp. 15–38, 2000.